Characterization of 260 GHz TES Bolometers for Detection of B-mode Polarization from the CMB

Alex Brinson
Mentors: Jamie Bock and Lorenzo Moncelsi

ABSTRACT

The Keck array is searching for evidence of Cosmic Inflation by searching for B-Mode polarization in the Cosmic Microwave Background (CMB). In order to subtract foreground signals from galactic dust and synchrotron emission, it is necessary to measure the B-mode polarization signal at multiple frequencies. New Transition Edge Sensor (TES) Bolometers designed to be sensitive at 260 GHz have been fabricated for use in the Keck Array. We characterized properties of these detectors relevant to CMB polarization measurement: optical efficiency, spectral response, and angular response. Optical efficiency is obtained by recording the power input from a blackbody source at room temperature, and at the boiling point of liquid Nitrogen (77K). Spectral response is found by Fourier-transforming the interference pattern from a Martin-Puplett interferometer. Angular response is estimated by near-field beam mapping an optically chopped signal, and comparing the power received by the detectors at different positions of the source. Analysis suggests that the new 260 GHz TES bolometers perform within the tolerance levels demonstrated by older, lower frequency sensors. The detectors are expected to begin scanning the CMB by early 2017.

1. INTRODUCTION

Cosmic inflation is a set of theories which attempts to explain the expansion of the universe as early as 10^{-32} seconds after the Big Bang {Guth, 1981}. If true, Inflation would provide explanations for many unexplained phenomena in early universe cosmology such as the flatness problem and the horizon problem {Boyanovsky, 2009; Guth, 1981}. It is believed that studying the vector field formed by the polarization of the Cosmic Microwave Background (CMB) could provide evidence for inflation in the form of B-modes. The polarization vector field can be decomposed into a basis of two orthogonal modes (Fig. 1): E-modes (Curl-free) and B-modes (Divergence-free) {Chiueh, 2001}. While scalar/density fluctuations in the early universe produce E-modes, which have already been detected to high significance, B-modes in the CMB can only originate from primordial gravitational waves (tensor fluctuations), such as those that would have been generated by Inflation { Krauss, 2010} ., at the surface of last scattering when the CMB formed. Therefore, a convincing detection of primordial B-mode polarization of the CMB would provide direct evidence in support of Inflation.

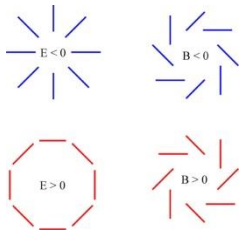

Fig. 1. — E-Modes and B-Modes
Examples of fields composed of purely E-mode (left), or purely B-mode (right). Though these modes are defined by a transformation of the Stokes parameters, E-modes can be viewed as curl-free, while B-modes are divergence-free. Blue indicates negative polarization, while red is positive.

In 2014, BICEP2 announced the detection of B-mode polarization {Ade, 2014 B}, but further analysis suggested that galactic dust in the foreground was largely (if not completely) responsible for the reported signal {Ade, 2015 a}. In order to avoid false positives from foreground sources such as dust and synchrotron, future CMB polarization surveys will need to record polarization data for several different frequency bands. Because the frequency dependence of the CMB is very different from that of dust or synchrotron {Krachmalnicoff, 2016}, sampling the aggregate signal at a variety of frequencies should make it possible to disentangle the individual components making up the sky signal and search for B-mode polarization from the CMB alone. The BICEP (Background Imaging of Cosmic Extragalactic Polarization) and Keck Array projects are currently probing the CMB with detectors designed to operate at 95, 150, and 230 GHz {Ade, 2015 d}. New detectors with a frequency band centered at 260 GHz have already been designed and fabricated, and are now being characterized in the lab before they can be deployed to the South Pole for use in CMB polarization measurements.

To fully characterize the 260 GHz detectors, we measured their spectral response, optical efficiency, and their angular response. We test optical efficiency by comparing the power responses from a black-body at two different temperatures. Frequency response is measured by using a Martin-Puplett interferometer and Fourier transforming the interferogram into a power spectrum for frequency {Ade, 2014 A}. Finally, the detectors' angular response is determined by performing near-field beam mapping with an optically chopped heat source that is scanned above the detectors, but outside the cryostat.

2. Transition Edge Sensors

Transition Edge Sensors (TES) are very sensitive to small changes in temperature because they take advantage of a material's superconducting phase transition {Bock, 1997}. At temperatures well below the critical temperature, the material is superconducting and has practically zero resistance. At temperatures well above the critical temperature, the material will have ordinary temperature dependence with its resistance. Within the transition range, however, the R vs. T curve is approximately a line of very large slope. By voltage-biasing the TES such that its temperature lies within the transition range (see TES Diagram), we can determine the external power input to the detector by measuring its change in resistance.

The TES is placed in parallel with a shunt resistor. When the detector is heated, the TES resistance increases and its current decreases. This current drop is measured by a superconducting quantum interference device (SQUID) that is coupled to an inductor placed in series with the TES (See TES Circuit).

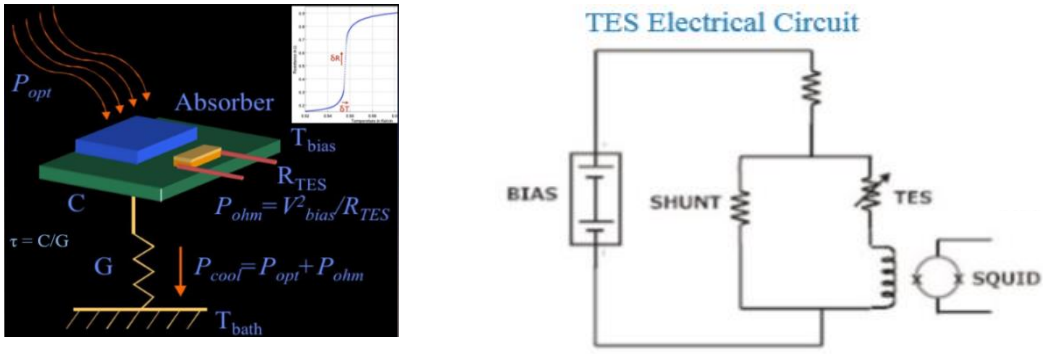

Fig. 2. — TES Diagram and Circuit

Left: Graph in upper left corner shows temperature dependence of a resistor around its phase change. Rest of diagram summarizes electrical and thermal connections to the sensor.
Right: Wiring schematic for a TES bolometer. Not shown is the entire chain of SQUIDs, which feedback on each other and keep the system in equilibrium.

BICEP and the Keck Array use TES bolometers made from Titanium and Aluminum {Ade, 2015 d} in order to observe the CMB. Aluminum transitions at a higher temperature than Titanium, so the former is used in lab to test various properties of the detectors without saturating them. Titanium is more sensitive due to its lower transition temperature and is used to collect actual polarization data at the South Pole.

Each TES bolometer receives power from a beam-forming array of slot antennas {Ade, 2015 d}, which collect light from the CMB. The TES bolometer is weakly thermally coupled to the 300mK thermal bath, and the sensitivity improves with the square root of the weakness of that thermal link. Detectors are arranged in an array of orthogonally polarized antenna pairs (see Detector Array), allowing for independent measurement of each direction of polarization.

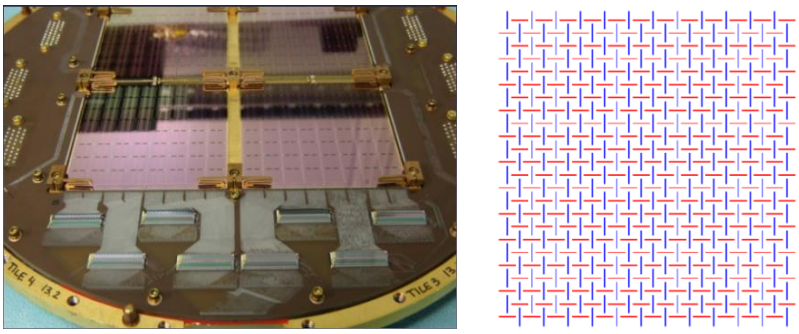

Fig. 3. — Detector Array

Left: Picture of focal plane. The quadrants are made of a grid of slot array antennas, each of which is thermally coupled to its own TES.
Right: Pattern of slot array antenna orientation. Antennas are arranged like this to create co-centered orthogonal detector pairs.

3. METHODS

3.1. Frequency Response:

Spectral response is measured by operating a Martin-Puplett interferometer above the apparatus window {Ade, 2014 A}. The Martin-Puplett interferometer has a small chamber filled with liquid Nitrogen, which acts as a black-body source. The randomly polarized light from this source reaches a linear polarizer, which splits the light into two orthogonally polarized beams. One beam is reflected at a fixed distance from the polarizer. The other beam is reflected by a motorized mirror, which travels at a constant velocity relative to the. Both beams are then reflected down to the focal plane, where they converge and produce interference patterns vs time, as recorded by the detectors.

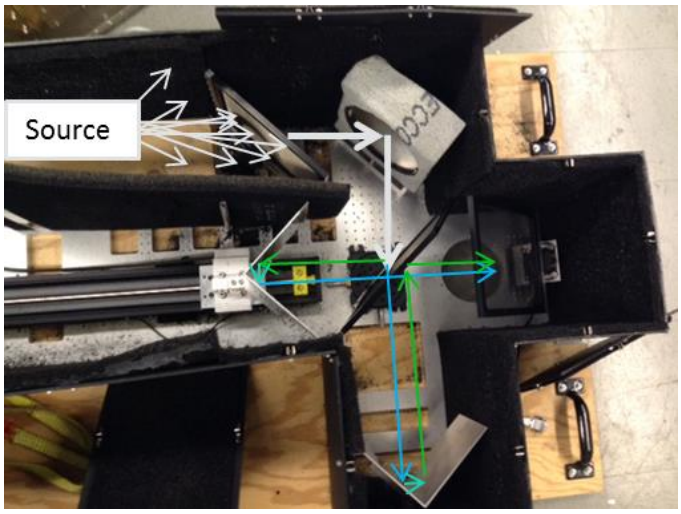

Fig. 4. — Martin Puplett Interferometer

Martin-Puplett interferometer used to collect spectral response data for the 260 GHz detectors. Starting from the top left, light from the source is collimated, reflected towards the polarizing lens, and then split into two polarized beams. The beam that reflected off the polarizing lens is then reflected by the moving mirror. The other beam is reflected by the bottom stationary mirror.

The interference between the two beams at the location of a detector is determined by the instantaneous path length and the wavelength of the light rays that are interfering. The resulting time-stream of data is known as an interferogram. A Fourier transform is performed on the interferogram to find the intensity vs. frequency spectrum for the detected light. By comparing this spectrum to the theoretical black-body spectrum, it is possible to infer the response of the detectors as a function of the input light's frequency.

Comparing the spectral responses across a pair of orthogonally polarized detectors is important for reducing the amount of systematic error in our CMB polarization data. If one detector has a different spectral response than its orthogonal counterpart, then the net polarization recorded by the detector pair will be artificially tilted towards one axis, and this will need to be accounted for in the analysis {Ade, 2015 d}.

We also want to estimate the band center and bandwidth of the detectors: If the detector's bandwidth is too small, they will collect CMB polarization data very slowly because they are sampling a tiny fraction of the total signal; if the bandwidth is too large, then the polarization data will add a large amount of uncertainty to the regression (for composite B-mode signal vs. frequency). In addition, the spectral response behavior plays an important role in our analysis for optical efficiency. For our goals, a bandwidth around 30% is desirable.

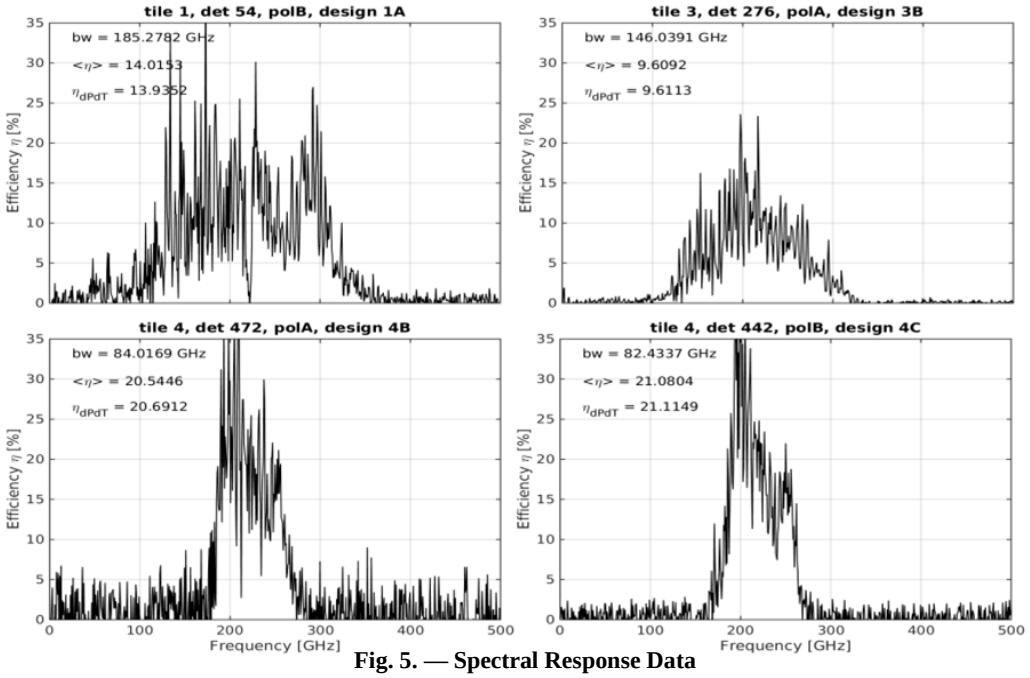

Fig. 5. — Spectral Response Data

Optical Efficiency vs. frequency plots for four different detectors. Bandwidth estimates (in GHz) are given for each detector as bw. The detectors behave differently because each has a distinct design.

3.2. Optical Efficiency:

To measure the optical efficiency, a black-body is placed above the vacuum window of the cryostat at room temperature (~300K), which causes each TES bolometer to receive an input power as described by the source's black-body spectrum within the frequency range where the detectors are responsive. Over a period of about 1 minute, the voltage bias for each detector is slowly ramped up, causing the detectors to heat up until the Aluminum portion of the TES goes from superconducting into its transition phase. Next, the source is cooled by filling it with liquid Nitrogen, bringing it to approximately 77K, and the voltage bias is once again ramped up until the TES's reach their transition phases. Because the source is cooler the second time, we expect a larger voltage bias to be necessary for the aluminum to begin transitioning. By transforming the bias ramping plot into a power vs. resistance plot, it is clear that within the transition phase there is a nearly constant difference in power between the two temperatures for a given resistance. By dividing this difference by 300K-77K = 223K, we obtain an experimental estimate of the power absorber per unit temperature difference ($\frac{dP}{dT}$) for each sensor.

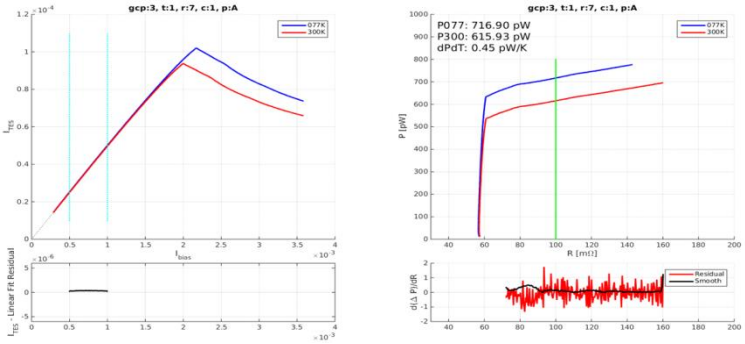

Fig. 6. — TES Optical Efficiency Data

Left: Plot showing current through TES as a function of the bias current for a blackbody source at 300K (red), and at 77K (blue). Until the aluminum reaches its transition point, the TES current scales linearly with the bias current. After this point however, the TES resistance will increase, and so its current will fall. The detector requires a larger bias current to reach its transition phase at 77K.

Right: Plot of power absorbed vs. resistance for the same process. The difference in power between the temperature curves is roughly constant once the detector begins transitioning.

Since we are working in the Rayleigh-Jeans limit where $hv \ll kT$, we know that $P_{opt} = kT\eta\,\Delta v$, where P_{opt} is the optical power received by the detector, k is Boltzmann's constant, T is the temperature, Δv is the bandwidth (as determined by spectral response analysis), and η is the optical efficiency {Ade, 2014 A}. This gives us the theoretical result that $\frac{dP}{dT} = k\eta\,\Delta v$, so we can use our experimental $\frac{dP}{dT}$ estimates to compute the optical efficiency for each detector as: $\eta = \frac{dP}{dT}\frac{1}{k\,\Delta v}$. An average optical efficiency between 30 and 40 percent is generally considered sufficient {Ade, 2015 d}.

3.3. Angular Response:

Angular response describes the dependence of detector sensitivity on the angle that the source makes with the optical axis. Angular response is characterized with a process called near-field beam mapping. A heat source capable of being moved vertically and horizontally is placed above the array window. The heat source is given a signature frequency by optically chopping it (We set it to 35 Hz). The source is moved to 1600 different positions on a 40 x 40 grid above the window. At each position, the source is held for 3 seconds while the TES bolometers record a time stream of the input power. There are many sources of noise that affect the power received by each detector, but the heat source signal can be identified by isolating the portion of the signal with the signature frequency.

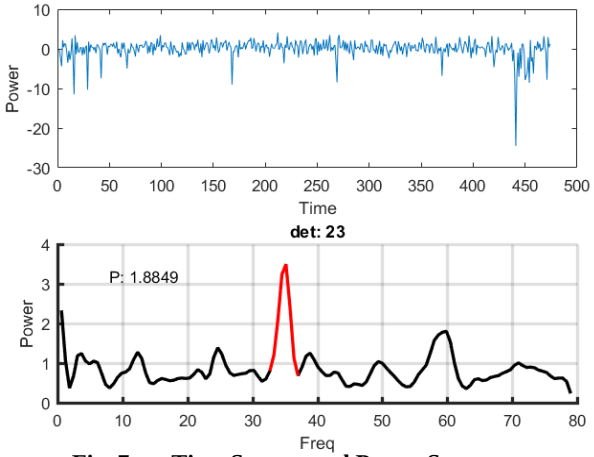

Fig. 7. — Time Stream and Power Spectrum

The top plot shows the power recorded by detector 23 as a function of time (units are not seconds; they are related to the detector sampling rate). It is very difficult to determine identify the heat source in the time stream.

The bottom plot shows the same data after it was transformed into a power spectrum. Because we chopped the heater at ~35 Hz, we know that the red portion of the spectrum is from the source, so we estimate the integral of the corresponding range as the total power measured by the detector at the given source position.

Once all 1600 runs are complete, we can construct a 40 x 40 pixel intensity map for each detector in the array. Maps for detectors are compared in later analysis to determine if the orthogonally polarized detectors in a pixel pair have sufficiently similar angular response.

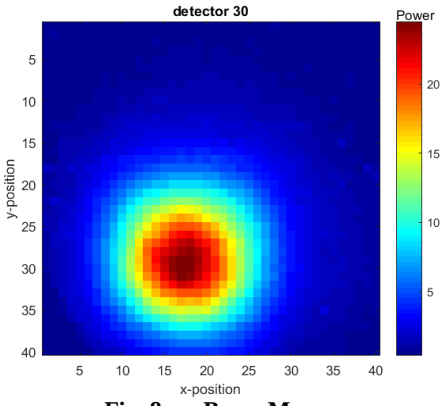

Fig. 8. — Beam Map

We record the power at every source position to construct an intensity map for each detector. The map for detector 30 looks promising, but we won't know how good it is for measurement until we fit the map and compare it to the detector it's paired to.

For a good bolometer, the intensity is greatest when the source is directly above the detector, then falls off radially as the off-axis angle is increased. Because the detectors are arranged in orthogonally polarized pairs, it is desirable for a pair of detectors to have very similar angular responses. If this is not the case, then it is possible for temperature to "leak" into a polarization measurement {Ade, 2015 b}

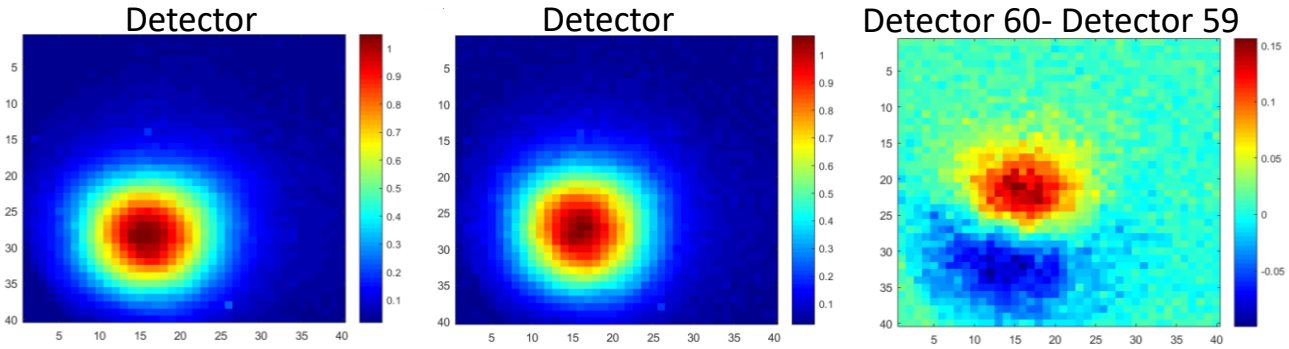

Fig. 9. — Angular Response Comparison for an Orthogonally Polarized Detector Pair

Though the beam maps for detectors 59 (left) and 60 (middle) appear very similar, subtracting one detector map from the other reveals a small disagreement in detector behavior (Right). This could introduce a significant artificial B-mode signal to the data if it is not properly accounted for.

since one polarization detector will be more sensitive than the other at a specific angle.

4. ANGULAR RESPONSE ANALYSIS

For every detector's beam map, we estimate the relevant response parameters by attempting to fit a two-dimensional Gaussian to the map intensity {Ade, 2015 b}. The relevant quantities are the horizontal and vertical center coordinates, the major and minor axis lengths, and the angle that the major axis makes with horizontal. If a beam's parameter estimates from this process do not make any sense (e.g. the beam center is off the map) or if the reduced chi-squared value from the fit is too large, then the detector is thrown out of the rest of the analysis, because it is likely that the detector was not operating correctly when the test was performed. Of the 528 detectors present in the array, only 217 of them

yielded beam maps that passed these fit requirements. It is possible (and worth investigating further) that some beam maps with sufficiently ideal shapes were incorrectly rejected due to a poor fit solution.

With these fit parameters, the angular responses for a pair of orthogonally polarized detectors can be compared quantitatively. If a discrepancy is found in a bolometer pair, then the effects on CMB polarization data can be accounted for in the analysis.

There are multiple ways in which the beam shapes of detectors can vary. Gain mismatch, differential pointing, differential beam width, and differential ellipticity are all types of detector pair response discrepancies that can be observed with near-field beam mapping {Ade, 2015 b, c}.

Unfortunately, the angular response analysis for the 260 GHz TES bolometers is still incomplete, because we were unable to compare fit parameters for paired detectors in time. We are able to see how far each individual detector deviates from an ideal angular response, but we are currently incapable of quantifying how much variation (and therefore systematic error) exists within an orthogonally polarized detector pair.

5. CONCLUSION

Though the analysis is still far from complete, it appears that there are a substantial number of detectors which do not respond ideally enough to record useful CMB data. This problem was made apparent in the near-field beam map fitting, where it was found that only 217 detectors satisfied the ideal beam shape requirements. The issue is further exacerbated by the fact that detectors must operate in pairs, so the proportion of detector pairs that could feasibly scan the CMB is likely even smaller. This was to be expected though, because we were characterizing a test focal plane that contained 8 different detector designs. The primary goal for this focal plane is to determine which designs perform the best for detecting around 260 GHz ; it is not intended for deployment to the South Pole.

There is still a sizeable quantity of detectors that work very well, so even if though this particular focal plane is not suitable for scientific measurement, it demonstrates that 260 GHz TES bolometers are certainly viable. Furthermore, by investigating which detectors work most effectively, we can refine the designs for future bolometers, allowing for future fabrication of higher performance, South-Pole-Worthy 260 GHz focal planes.

REFERENCES

Ade, P.A., Aghanim, N., Ahmed, Z., et al., 2015, Phys Rev Lett 114(10): 101301. (a)

Ade, P.A., Aikin, R.W., Amiri, M., et al., 2014: 30. (A)

Ade, P.A., Aikin, R.W., Amiri, M., et al., 2015: 27. (b)

Ade, P.A., Aikin, R.W., Amiri, M., et al., 2015: 21. (c)

Ade, P.A., Aikin, R.W., Barkats, D., et al., 2014, Phys Rev Lett 112(24): 241101. (B)

Ade, P.A.R., Aikin, R.W., Amiri, M., et al., 2015, The Astrophysical Journal 812(2): 176. (d)

Bock, J.J., LeDuc, H.G., Lange, A.E., Zmuidzinas, J., & European Space, A., 1997, A monolithic bolometer array suitable for first. in Far Infrared and Submillimetre Universe: An Esa Symposium Devoted to the Far Infrared and Submillimetre Telescope, (European Space Agency, Paris, 349).

Boyanovsky, D., Destri, C., De Vega, H.J., & Sanchez, N.G., 2009, Int. J. Mod. Phys. A 24(20-21): 3669.

Chiueh, T.H., & Ma, C.J., 2001, Separation of E and B patterns in the local CMB polarization map. in Relativistic Astrophysics, ed J. C. Wheeler, & H. Martel (Amer Inst Physics, Melville, 208).

Guth, A.H., 1981, Physical Review D 23(2): 347.

Krachmalnicoff, N., Baccigalupi, C., Aumont, J., Bersanelli, M., & Mennella, A., 2016, Astronomy & Astrophysics 588: A65.

Lawrence Krauss, S.D., Stephan Meyer, 2010: 15.